AOARD REPORT

XV NSO/Sac Peak Solar Workshop held at Sunspot, New Mexico on 19-23 September 1994.

19-23 Sept 1994

Dr Y. Suematsu
National Astronomical Observatory

With financial support provided under the AFOSR sponsored Window-on-Science program, Dr Y. Suematsu, an astronomer at National Astronomical Observatory, Mitaka, Tokyo, Japan, presented a paper at XV NSO/Sac Peak Solar Workshop held at Sunspot, New Mexico on 19-23 September 1994. The report includes his technical overview of the workshop and details of the paper which he has presented at the workshop. His paper dealt with studies of line profile fitting analysis of He I 1083nm line spectra obtained by using a 25 cm aperture coronagraph at Norikura Solar Observatory in Japan.

AIR FORCE OFFICE OF SCIENTIFIC RESEARCH

ASIAN OFFICE OF AEROSPACE RESEARCH AND DEVELOPMENT

TOKYO, JAPAN
UNIT 45002
APO AP 96337-0007
DSN: (315)229-3212
Comm: 81-3-5410-4409

Report of the 15th Summer Workshop of the National Solar Observatory/Sacramento Peak

Y.Suematsu
National Astronomical Observatory, Mitaka, Tokyo 181

1. Overview

The National Solar Observatory at Sacrament Peak, New Mexico, has a tradition of bringing together both observers and theoreticians for productive interactions at these summer workshops. This summer's workshop was entitled: "IR tools for Solar Astrophysics: What's Next?" and focused on new developments in the infrared solar window, with emphasis on studies of the solar corona. The workshop was held from 19 to 23 September, 1994, and attended by about seventy scientists and engineers from many countries. It was indeed a productive and very enjoyable workshop. In the following, summaries of some major concerns of the workshop are given.

2. Observational Consequences of Competing Coronal Heating Models

From theoretical points of view, three mechanisms for heating the solar corona have been proposed: heating by acoustic or magnetohydrodynamic waves, by electric currents, and by the dissipation of turbulence. In order to attempt to descriminate between these mechanisms, it is useful to compute possible observational signatures of each models. These include volume filling factors, spectral line profiles, differential emission measures, count rates in high temperature lines, and signatures from energetic electrons. However, even with this information, there remain frustrating ambiguities that may be difficult to resolve.

3. IR Coronal Spectrum

Predicted infrared forbidden coronal emission lines were reviewed. The wavelength of Si X line was measured to be 1430.084 ± 0.006 nm and Fe XIII lines were located at 1074.617 ± 0.005 nm and 1079.783 ± 0.006 nm. These lines are very useful to derive coronal electron densities and magnetic field intensities.

In addition, it is likely that coronal IR line intensities can be deduced from abundant UV spectral lines when they share common upper atomic energy levels and the relevant Einstein A coefficients are known. It has been examined by Dr. Chang the intensities of a number of IR lines in Fe XIV, both forbidden and allowed. It was suggested that other IR lines from the excited states of ground configurations appear more promising.

4. IR Detectors

The development of two dimensional arrays for infrared astronomy began in the late 1970's with the General Electric 32×32 InSb (Indium Antimonide) Charge Injection device. However, the first truly utilitarian array, in terms of requisite performance for astronomical observations and availabilities to the astronomical community, was Santa Barbara Research Center (SBRC) 58×62 InSb array. It was soon followed by Rockwell NICMOS family of HgCdTe (MCT) arrays. Both companies utilized the source follower per detector (SFD) architecture and indium bump technology, which has become standard for all low background infrared focal planes. Low background infrared arrays use the SFD multiplexer design because CCD's do not perform well at the optimum detector operation temperature (30-70 K).

Within the past decade, three detector technologies, PtSi (Platinum Silicide), InSb, and MCT (Mercury Cadmium Telluride), have produced devices of interest to observational astronomers. With the

introduction of 1K×1K arrays in InSb and MCT interest in PtSi devices has waned due to its low quantum efficiency. It was discussed that the performance, advantages, and disadvantages of these materials. The current and next generation arrays, 256×256 and 1024×1024 InSb, and 1024×1024 HgCdTe, were introduced with promising performances.

5. IR Observations of Photospheric Magnetic Fields

Several groups are now measuring photospheric magnetic fields using the two Zeeman-sensitive Fe I lines near 1.56 μm. The scientific emphasis is shifting toward full Stokes polarimetry of sunspots and plages, and highly sensitive Stokes–V searches for intrinsically weak fields (¡ 500 G) in network and intranetwork areas. It is likely that the next generation of near-IR magnetographs will also concentrate on the 1.56 μm lines.

6. Solar Photospheric Structure with New IR Observations

A systematic analysis of the infrared CO lines (2.3 to 6.7 μm) with the Spacelab-3 ATMOS experiment was carried out. The line-center brightness temperatures range from 4300 to 6300 K for the strongest to the weakest of these lines, respectively, and the depths of formation range from low chromospheric heights to deep in the photosphere. A close match to all of these lines with a single, hydrostatic equilibrium model was obtained. This model, however, is too cool in the outer layers to be consistent with other observations in the UV, that show sensitivity to the temperature increase in the chromosphere. A few atmospheric models were presented and discussed to be reconciled with this problem. On the other hand, eclipse measurement of CO and Pfund H(7-5) emission distribution above the solar limb clearly showed that these lines extends only about 0.55 arcsec beyond the continuum limb, indicating that cool atmosphere of at least 400 km thickness exists above temperature minimum layer.

7. He I λ1083nm Line Observations

The He I 1083nm line is an indicator of both coronal and chromospheric dynamics. The coronal signature arises due to the excitation of the helium atom to its 3S (19.6eV) state by back radiation from coronal UV lines. Thus changes in the coronal UV intensities would be expected to be manifested as changes in the amount of He I 1083nm absorption. The chromospheric signature could possibly arise due to an increase in the number of absorbing atoms in the line of sight either by a change in the plasma density or by collisional excitation caused by enhancement of temperature. At the workshop, new results on wave properties and magnetic field measurements in the He I 1083nm line were presented and discussed.

8. Large (2-4m) Reflecting Coronagraphic Telescope

Infrared solar astronomy is severly limited by the telescopes and instrumentation available. The largest full-wavelength coverage IR telescope is the 150 cm McMath-Pierce facility on NSO/Kitt Peak. Its diffraction limited angular resolution is inadequate for many solar uses at the longer wavelengths and it suffers from seeing at shorter wavelengths. An upgrade to a 4 meter aperture combined with seeing at inprovements and rapid guiding techniques is being considered.

The 240 cm Large Earth-Based Solar Telescope (LEST) presents another option for enhanced IR capabilities. Its entrance window, however, limits the wavelength coverage to 0.3-2.5 μm. All-reflecting coronagraphs (largest available is 50 cm) suffer similar wavelength coverage limitations. Reflecting coronagraphs are being developed which would allow both full wavelength coverage, achromatism, and larger apertures to enhance both angular resolution and photon gathering.

From these considerations, the preliminary design of the NSO Large Reflecting Coronagraph was presented at the Workshop: The optics are near diffraction- limited, and are expected to provide excellent imaging over small (several arcsec) field of view, and slightly degraded imaging over larger (1 deg) field of view. The system employ inverse occulting in the prime focal plane using mirrors of various shapes and sizes to reject unwanted light associated with bright sources in close proximity to faint objects which are

otherwise difficult to observe. Active correction is achieved via both tilt and phase-correcting mirrors. Its low scattered light and low IR emissivity characteristics would make this 2 to 4 meter aperture telescope very attractive for both disk and corona studies and for both day and night time observations.

He I λ1083nm OBSERVATIONS AND CHROMOSHERIC AND CORONAL ACTIVITIES

Y. Suematsu, K.Ichimoto, and T.Sakurai

National Astronomical Observatory of Japan, Mitaka, Tokyo 181, Japan

Abstract

We present some results on studies of line profile fitting analysis of He I 1083nm line spectra which were obtained with a 25-cm aperture coronagraph at the Norikura Solar Observatory.

1. Introduction

The He I 1083nm line is a good indicator of both coronal as well as chromospheric structures and activities. Since 1989, we have obtained a number of spectra and spectroheliograms of this useful line at the Norikura Solar Observatory. From these data, we have found: a close relationship between the steady structures in He I 1083nm intensity, velocity fields, and photospheric magnetic fields, many dark points in active regions which vary with a time scale of 10–20 min, and various manifestations of flares in this line (Hiei et al. 1991; Ichimoto et al. 1993). Here we present some results of line-profile fitting analysis of this line.

2. Observations

The spectra were obtained with a CCD camera (512×480 pixels), mounted on one of the exits of Littrow-type spectrograph. The solar image was scanned so as to give full disk spectroheliogram; it consists of four scannings in east-west direction. One pixel corresponds to 1.08 arcsec in spatial direction and 0.097Å in dispersion direction. Two parts of wavelength range were usually recorded: One is 1.75Å band centered on 10830.3Å and the other is 0.68Å band at its nearby continuum of 10834Å.

3. Method of Line Profile Fitting

We assumed that the He I λ1083nm line profiles are given by (e.g. Avrett et al. 1994),

$$I(\lambda) = I_c \; exp(-\tau(\lambda)) + S(1 - exp(-\tau(\lambda))),$$

where $I(\lambda)$ is the intensity in He I λ1083nm, I_c is a continuum intensity near the line, S is the source function of the line, and

$$\tau(\lambda) = \tau_0 \; exp(-(\lambda - \lambda_0)^2/\Delta\lambda_D^2),$$

where τ_0 is the optical thickness of line center, λ is the Doppler shifted wavelength, and $\Delta\lambda_D$ is the Doppler width. Here, The S is assumed to be constant and 0.4 times I_c (cf. Avrett et al. 1994; Giovanelli and Hall 1977).

The observed profile is normalized by the nearby continuum and we have reduced profile given by

$$C(\lambda) = (I(\lambda) - I_c)/I_c,$$

Then, we can express the reduced profile with the following equation;

$$C(\lambda) = (S/I_c - 1)(1 - exp(-\tau(\lambda))),$$

We obtained with nonlinear least square fitting procedure the three unknown parameters of τ_0, λ_0, and $\Delta\lambda_D$, which specify physical and dynamical properties of the He I λ1083nm chromosphere. Equivalent width was calculated from the fitted line-profile, because the observation gave only small part of line-profile.

4. Results

We studied the relationships between line-profile parameters obtained. He I λ1083nm line is weak and the observed profiles were noisy, and so we selected good fittings which were defined as that standard deviation of fittings divided by line depth is less than 5%. Scatter plots between line-profile parameters for the data of September 3, 1994 are shown in Figures 3 and 4. Results for other dates were almost the same as those presented here.

(1) Equivalent widths (EW) are in the range of 0.02 to 0.2Å. We tentatively classify the region by the number of EW and optical thickness (or line depth) (cf. Jones 1994); quiet region where τ_0 is less than 0.1 has EW less than 0.1, active region has EW between 0.1 and 0.2, and filament has EW between 0.05 and 0.15 where the optical depth is large 0.15–0.3 and Doppler width is small (about 0.5Å).

(2) We have large scatters in EW–Doppler width (DW) relations. Especially it is large in quiet region. This is partly because of poor fittings there and partly because of randam motion of spicules (cf. Venkatakrishnan et al. 1992). It is interesting to suggest that large DWs are associated with overlying coronal heatings (Venkatakrishnan 1993), although in order to confirm this, we need further information.

(3) Large Doppler shifts up to 10 km s^{-1} (0.4Å) are seen in quiet region which might indicate the upward motion of spicules.

We have seen that the He I 1083nm line give us sensitive diagnostics of coronal and chromospheric phenomena. We are planning to have a filter system ($LiNbO_3$ Fabry-Perot type) for this useful line to increase time resolution in the near future.

References

Avrett, E.H., Fontenla, J.M., and Loeser, R.: 1994, *IAU Symp.* **154**, "Infrared Solar Physics", p.35, Kluwer Academic Pub.

Jones, H.P.: 1994, *IAU Symp.* **154**, "Infrared Solar Physics", p.49, Kluwer Academic Pub.

Giovanelli, R.G. and Hall, D.: 1977, *Solar Phys.* **52**, 211.

Hiei, E., Ichimoto, K., and Fang, G.:1991, "Flare Physics in Solar Activity Maximum 22", *Lecture Note in Phys.* **387**, 67.

Ichimoto, K., Fang, G., and Hiei, E.:1993, "Proc. of the First China-Japan Seminar on Solar Physics", p.158, Kunming TonDar Institute.

Venkatakrishnan, P. et al.: 1992, *Solar Phys.* **138**, 107.

Venkatakrishnan, P.: 1993, *Solar Phys.* **148**, 233.

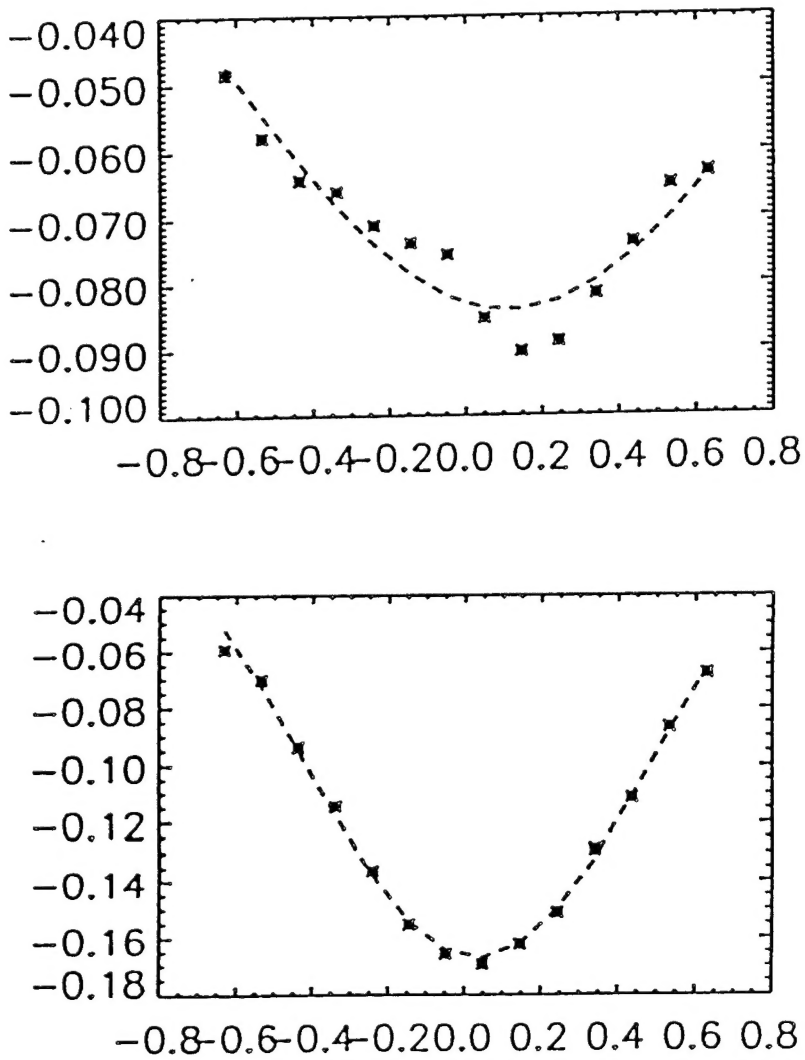

Fig. 1 Examples of line-profile fittings of He I λ1083nm line.

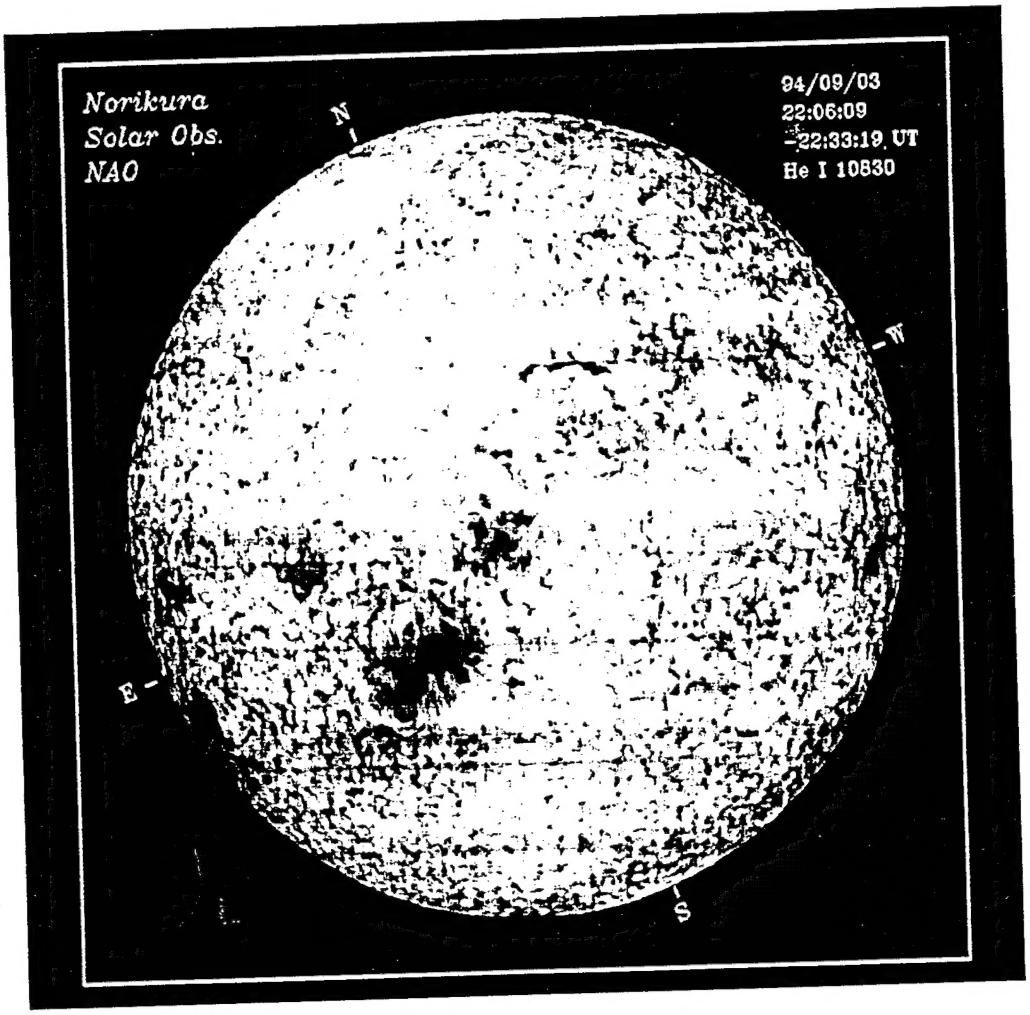

Fig. 2 He I λ1083nm spectroheliogram on September 3, 1994.

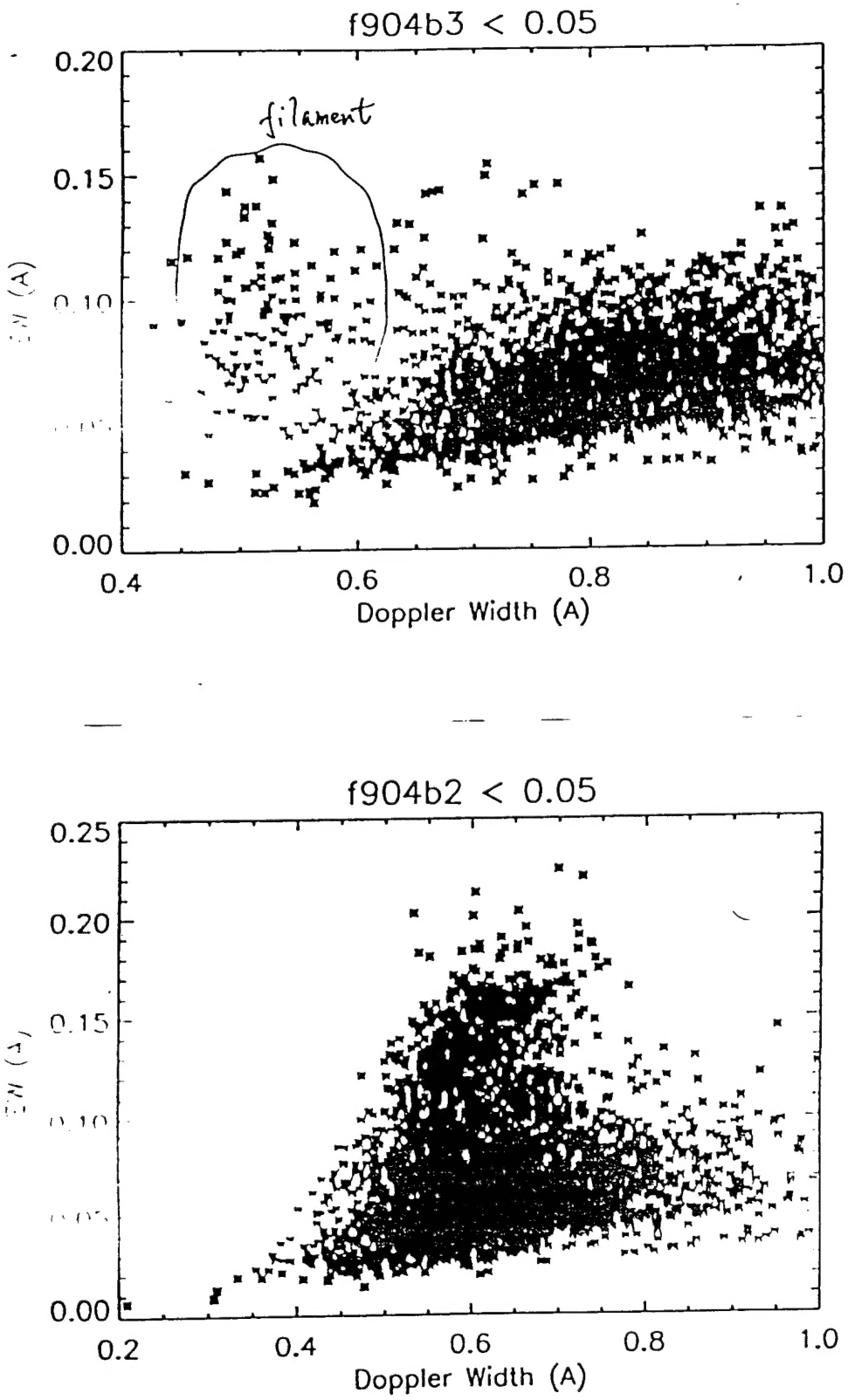

Fig. 3 Scatter plots of equivalent widths vs. Doppler widths of He I λ1083nm line for the data of Sep. 3, 1994. The upper panel is for north (quiet and filament region) and the lower for south hemisphere (active region).

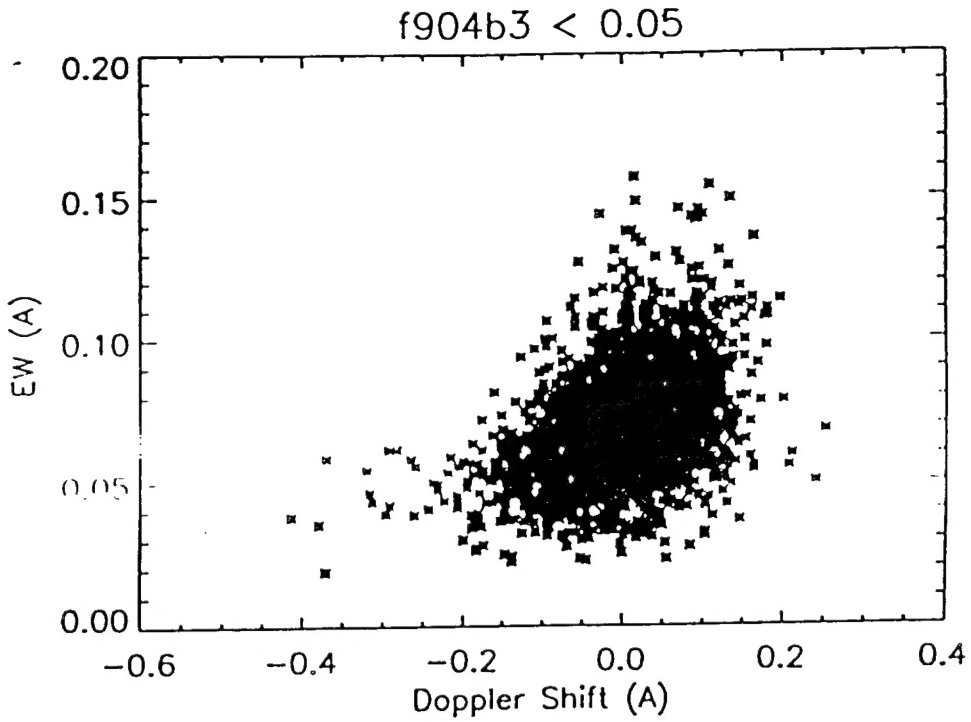

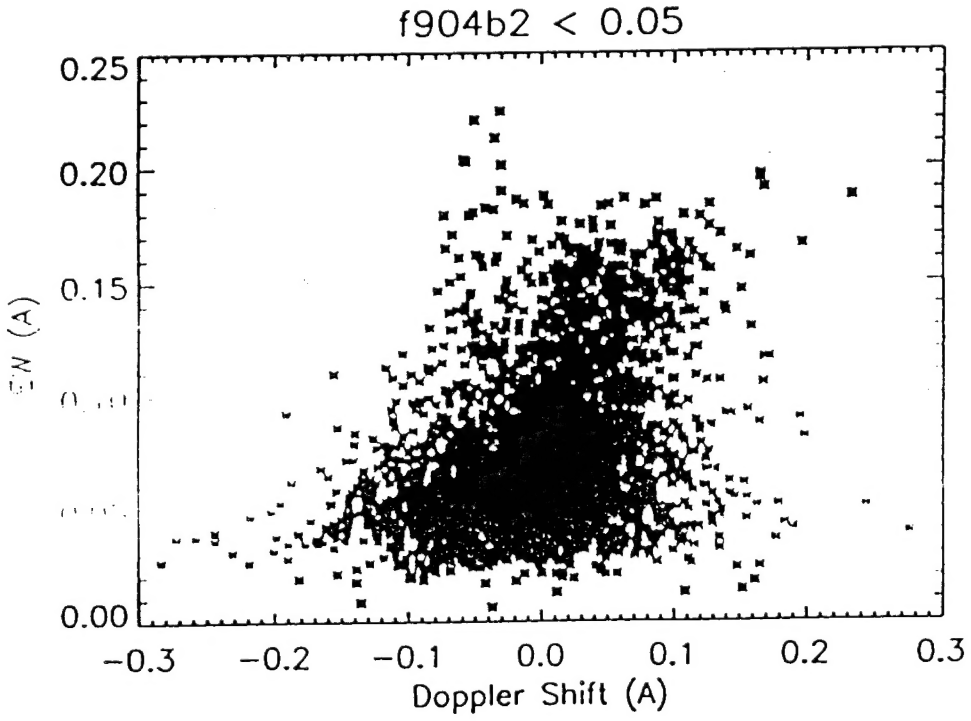

Fig. 4 Scatter plots of equivalent widths vs. Doppler shifts of He I λ1083nm line for the data of Sep. 3, 1994. The upper panel is for north (quiet and filament region) and the lower for south hemisphere (active region).